Journal of Materials Chemistry A

ROYAL SOCIETY OF CHEMISTRY

PAPER

View Article Online
View Journal | View Issue

Cite this: J. Mater. Chem. A, 2021, 9, 21151

"Thiol–ene" click synthesis of chiral covalent organic frameworks for gas chromatography†

Jing-Xuan Guo, [abcd] Cheng Yang [abc] and Xiu-Ping Yan *[abcd]

Received 1st June 2021
Accepted 16th August 2021

DOI: 10.1039/d1ta04621g

rsc.li/materials-a

The unique properties of covalent organic frameworks (COFs), such as a large specific surface area, good stability and easy functionalization, make them have good potential in the field of separation science. However, the synthesis of chiral COFs is challenging, so the application of COFs in chiral separation is very limited. Here, we show a simple and effective "thiol–ene" click strategy to construct chiral COFs. The chiral COF CTzDva showed high thermal stability and good porosity, prompting us to explore its application in chromatographic separation. The CTzDva-based gas capillary column showed good separation of benzene/cyclohexane, and racemates (citronellal and fenchone). This work provides a promising platform for the synthesis of chiral COFs and expands the application of COFs in the field of separation.

Introduction

As a new type of porous crystalline material, covalent organic frameworks (COFs) have attracted significant interest due to their unique structures and excellent properties such as a large specific surface area, adjustable pore structure, easy control of functions and good stability.[1–6] Recently, COFs have been widely used in diverse fields such as gas adsorption and storage,[7,8] catalysis,[9,10] sensing,[11,12] drug delivery[13,14] and separation.[15–19]

Chiral enantiomers have identical physical or/and chemical properties, but may possess completely different biological activities, pharmacology and toxicity, so the separation of chiral enantiomers is of great significance and challenge.[20–22] Chromatography based on a chiral stationary phase is an efficient technique for chiral separation.[23–27] Recently, chiral COFs have been explored as novel stationary phases in chromatography for chiral separation.[28–30] In 2016, Qian *et al.* proposed a bottom-up strategy to prepare chiral COFs for gas-phase chromatography (GC) separation of enantiomers (±)-1-phenylethanol, (±)-1-phenyl, (±)-1-propyl alcohol and (±)-limonene.[28] Subsequently, Ma and Cui prepared chiral COFs for high performance liquid chromatography (HPLC) separation of racemes.[29,30] These pioneering studies demonstrate the good prospects of chiral COFs in chiral separation. Even so, the application of COFs in the separation of enantiomers is still in the exploratory stage.

The synthesis of chiral COFs is very challenging because the balance between asymmetry and crystallinity should be fully considered in their preparation.[31] Post-synthetic modification has been extensively used to design functionalization on the preformed frameworks of COFs.[32–34] The introduction of reactive chemical groups into the COF framework is an effective way to construct functional COFs for specific applications. The "thiol–ene" click reaction is a kind of simple and efficient chemical reaction, which is often used in the functionalization of materials.[35–38]

Herein, we report a simple "thiol–ene" click strategy for the construction of a new chiral COF and its capillary column for chiral GC separation. 2,5-Divinyl-1,4-benzaldehyde (Dva) with C=C double bond reaction sites is selected as the monomer to condense with 2,4,6-tri(4-aminophenyl)-1,3,5-triazine (Tz) for the synthesis of a new vinyl functionalized COF TzDva as the precursor COF. Subsequently, chiral sulfur derivatives (*R*)/(*S*)-*N*-(2-mercaptoethyl)-2-phenylpropanamide were synthesized to bind with TzDva *via* the "thiol–ene" click reaction to synthesize chiral COF CTzDva. The prepared CTzDva shows high thermal stability and good porous properties. Furthermore, the fabricated CTzDva coated capillary column enables chiral separation of the racemates of citronellal and fenchone. This work provides a promising way to develop chiral COFs for chiral related applications.

Experimental section

Chemicals and reagents

All chemicals and reagents used are at least of analytical grade. Tz was supplied by Bide Pharmatech Ltd. (Shanghai, China).

[a]State Key Laboratory of Food Science and Technology, Wuxi 214122, China. E-mail: xpyan@jiangnan.edu.com

[b]International Joint Laboratory on Food Safety, Jiangnan University, Wuxi 214122, China

[c]Institute of Analytical Food Safety, School of Food Science and Technology, Jiangnan University, Wuxi 214122, China

[d]Key Laboratory of Synthetic and Biological Colloids, Ministry of Education, Jiangnan University, Wuxi, 214122, China

† Electronic supplementary information (ESI) available. See DOI: 10.1039/d1ta04621g

Dva was purchased from Kaiyulin Pharmaceutical Technology Co. Ltd. (Shanghai, China). 2-Aminoethyl mercaptan, (+)-citronellal and (+)-fenchone were purchased from Energy Chemical (Shanghai, China). (−)-Fenchone and (−)-citronellal were purchased from Macklin Biochemical Co. Ltd. (Shanghai, China). Deuterium chloroform ($CDCl_3$), 2-phenylpropionic acid, (*R*)-(−)-2-phenylpropionic acid and (*S*)-(+)-2-phenylpropionic acid were purchased from J&K Scientific Co. Ltd. (Beijing, China). Scandium(III)trifluoromethanesulfonate ($Sc(OTf)_3$), mesitylene, 1,4-dioxane, 2-pentanone, 1-nitropropane, pyridine, benzene, *n*-undecane, *n*-dodecane, *N*-hydroxysuccinimide (NHS), 1-(3-dimethylaminopropyl)-3-ethylcarbodiimide hydro (EDC), vinyltrimethylsilane, *o*-dichlorobenzene (o-DCB), *N*,*N*-dimethylacetamide (DMAC), 2,2-azobisisobutyronitrile (AIBN) and *n*-butanol were obtained from Aladdin Chemistry Co. Ltd. (Shanghai, China). Cyclohexane, normal alkane (n = 5–10), tetrahydrofuran (THF), acetonitrile (ACN), ethanol (EtOH), methanol (MeOH), dichloromethane (DCM), *N*,*N*-dimethylformamide (DMF), toluene and acetone were provided by Sinopharm Chemical Reagent Co. Ltd. (Shanghai, China). Ultrapure water was obtained from Wahaha Foods Co. Ltd. (Hangzhou, China).

Instrumentation

Powder X-ray diffraction (PXRD) patterns were obtained on a D2 PHASER diffractometer (Bruker AXS GmbH, Germany) with CuK_α radiation in the range of 2–40° with a scanning speed of 6° min^{-1}. Fourier transform infrared (FT-IR) spectra were recorded on a Nicolet IS20 spectrometer (Nicolet, USA). Thermogravimetric analysis (TGA) was performed on a PTC-10A thermogravimetric analyzer (Rigaku, Japan). Scanning electron microscope (SEM) images were recorded on an SU8100 scanning electron microscope (Rigaku, Japan). Transmission electron microscopy (TEM) images were acquired on a JEM-2100 transmission electron microscope (Rigaku, Japan). N_2 adsorption experiments were performed on an Autosorb-iQ analyzer (Quantachrome, USA). X-ray photoelectron spectroscopy (XPS) spectra were recorded on an Axis supra spectrometer (Kratos, MA, UK) with monochromatized AlKα radiation ($h\nu = 1486.6$ eV, 225 W) as an X-ray source. ^{1}H and ^{13}C nuclear magnetic resonance (NMR) spectra were recorded on an AVANCE III HD 400 MHz NMR spectrometer (Bruker, Switzerland). Circular dichroism (CD) spectra were recorded on a Chirascan V100 (Applied Photophysics, England). The specific rotations were recorded on an Autopol IV polarimeter (Rudolph, USA). GC measurements were performed on a Shimadzu 2010 Plus system with a flame ionization detector (FID) with nitrogen (99.999%) as the carrier gas.

Synthesis of chiral thiol derivatives

(*S*)-*N*-(2-Mercaptoethyl)-2-phenylpropionamide was produced by the esterification reaction of (*S*)-2-phenylpropionic acid and 2-aminoethanethiol (Fig. S1†). EDC·HCl (2.30 g, 12.00 mmol) and NHS (1.38 g, 11.99 mmol) were added to an acetonitrile solution (20 mL) of (*S*)-2-phenylpropionic acid (1.50 g, 10.00 mmol), and then the resulting mixture was stirred at room temperature in the dark for 4 h to yield the reactive ester of (*S*)-2-phenylpropionic acid. To the above mixture, 3.48 mL of DIPEA (19.98 mmol) and 1.54 g of 2-aminoethanethiol (20.00 mmol) were added in sequence and the resulting mixture was vigorously stirred at room temperature overnight. The solvent was then evaporated in a vacuum. After cooling to room temperature, 100 mL of ultrapure water was added. The resulting mixture was adjusted to weak acidity with HCl (1 mol L^{-1}) and extracted with DCM (50 mL). The obtained organic phase was then washed thrice with water alkalified to pH 9 with NaOH solution (1 mol L^{-1}). The organic phase was dried with anhydrous magnesium sulfate and concentrated to afford the titular compound (*S*)-*N*-(2-mercaptoethyl)-2-phenylpropanamide as a pale yellow thick liquid (yield: 63.1%, 1.32 g) (Fig. S1–S4†). ^{1}H NMR (400 MHz, $CDCl_3$) δ (ppm): 7.40–7.37 (m, 2H, Ar–H), 7.34–7.31 (m, 3H, Ar–H), 5.78 (s, 1H, –NH–), 3.60 (q, 1H, –CH–), 3.42–3.35 (m, 2H, $-CH_2-$), 2.64–2.58 (m, 2H, $-CH_2-$), 1.66 (s, 1H, –SH), 1.56 (d, 3H, $-CH_3$). ^{13}C NMR (100 MHz, $CDCl_3$) δ (ppm): 174.38, 141.30, 128.99, 127.62, 127.38, 47.09, 42.40, 24.50, 18.40. MS (ESI^-), m/z: $[M-H]^-$ calcd 208.09, found 208.00. FT-IR: –NH–CO– (1640 cm^{-1}). (*R*)-*N*-(2-Mercaptoethyl)-2-phenylpropanamide was synthesized from (*R*)-2-phenylpropionic acid in the same way (Fig. S4–S6†). ^{1}H NMR (400 MHz, $CDCl_3$) δ (ppm): 7.38–7.28 (m, 5H, Ar–H), 5.76 (s, 1H, –NH–), 3.57 (q, 1H, –CH–), 3.41–3.30 (m, 2H, $-CH_2-$), 2.61–2.56 (m, 2H, $-CH_2-$), 1.81 (s, 1H, –SH), 1.53 (d, 3H, $-CH_3$). ^{13}C NMR (100 MHz, $CDCl_3$) δ (ppm): 174.39, 141.29, 128.92, 127.56, 127.30, 46.98, 42.39, 24.43, 18.41. MS (ESI^-), m/z: $[M-H]^-$ calcd 208.09, found 208.10. FT-IR: –NH–CO– (1640 cm^{-1}).

Synthesis of TzDva

A 35 mL Schlenk tube was charged with Tz (28.3 mg, 0.08 mmol), Dva (22.3 mg, 0.12 mmol), and a mesitylene/1,4-dioxane solution (1 : 1 v/v, 1 mL), and the resulting suspension was sonicated for 10 min. Afterwards, $Sc(OTf)_3$ (2.4 mg, 4.8 μmol) was added, and the resulting suspension was sonicated briefly. Then, the tube was frozen in a liquid nitrogen bath, degassed through three freeze–pump–thaw cycles, and sealed with a screw cap, and the reaction mixture was kept at room temperature for 1 d. The yielded precipitate was collected by centrifugation and washed with THF several times. The collected powder was dried at 45 °C under vacuum for 12 h to afford TzDva with 95.5% isolated yield and a molecular formula of $(C_{12}H_{14}N_2)_n$.

Synthesis of CTzDva

To the mixture of TzDva (30 mg), (*S*)-*N*-(2-mercaptoethyl)-2-phenylpropanamide (50 mg), AIBN (3 mg), and THF (3.0 mL) were added into a 35 mL Schlenk tube. After stirring under a N_2 atmosphere at 70 °C for 24 h, the product was isolated by centrifugation, washed with THF, and dried under vacuum at 40 °C to afford (*S*)-CTzDva. (*R*)-CTzDva was synthesized from (*R*)-*N*-(2-mercaptoethyl)-2-phenylpropanamide in the same way.

Fabrication of the COF coated capillary column

A fused silica capillary (30 m long × 0.32 mm i.d., Yongnian Optic Fiber Plant, Hebei, China) was pretreated according to the

following recipe before dynamic coating: the capillary column was washed with NaOH (1 mol L^{-1}) for 2 h, ultrapure water for 30 min, HCl (0.1 mol L^{-1}) for 2 h, ultrapure water until the outflow reached pH 7.0 and methanol for 30 min. The capillary was then dried with N_2 at 100 °C overnight.

CTzDva was coated onto the pretreated capillary column *via* a dynamic coating method as follows: 0.5 mL ACN suspension solution of CTzDva (1.0 mg mL^{-1}) was first filled into the capillary column under gas pressure and then pushed through the column at a constant N_2 pressure of 10 kPa to leave a wet coating layer on the inner wall of the capillary column. To avoid the acceleration of the solution plug near the end of the column, a 4 m long buffer tube was attached to the capillary column end as a restrictor. After coating, the capillary column was settled under N_2 overnight. Further conditioning of the capillary column was carried out using a temperature program: 30 °C for 30 min, ramp from 30 °C to 240 °C at a rate of 10 °C min^{-1}, and 240 °C for 3 h. The preparation of the TzDva coated capillary column was performed in the same way as for the CTzDva coated capillary column except that EtOH was used to replace ACN as the dispersing solvent of TzDva.

Preparation of the (*S*)-*N*-(2-mercaptoethyl)-2-phenylpropanamide functionalized capillary column

A capillary column (30 m long × 0.32 mm i.d.) was washed with 1 mol L^{-1} NaOH for 2 h, and then rinsed with ultrapure water for 1 h, and 0.1 mol L^{-1} HCl for 2 h, and finally rinsed with ultrapure water until the effluent solution reached pH 7.0. A mixed solution of vinyltrimethylsilane and methanol (1/1, v/v) was injected into a dry capillary, while the two ends of the capillary were blocked. The capillary was placed in a 40 °C oven to react overnight, rinsed with methanol and dried under the protection of N_2 to obtain the vinyl functionalized capillary.

(*S*)-*N*-(2-Mercaptoethyl)-2-phenylpropanamide (50 mg) and AIBN (3 mg) were dissolved in 3 mL THF, and then injected into the vinyl functionalized capillary. After incubation in a 60 °C water bath for 24 h, the prepared capillary column was rinsed with THF to remove the residuals, and then flushed with N_2 for 2 h to remove the solvent. Finally, the prepared capillary column was conditioned with a temperature program: 60 °C for 30 min, ramp from 60 °C to 180 °C at a rate of 3 °C min^{-1}, and 180 °C for 2 h.

Results and discussion

Synthesis and characterization of TzDva and CTzDva

Fig. 1 shows the developed "thiol–ene" click strategy for the fabrication of chiral COFs. To construct the chiral COFs, the precursor COF TzDva was first synthesized *via* the imine condensation reaction of Tz and Dva. The triazine group of the Tz monomer has a good rigid planar structure for the formation of an ordered structure of COFs, while the Dva monomer provides a vinyl group to facilitate the subsequent reactions. Subsequently, the obtained TzDva and chiral thiol derivative were reacted in a suitable solvent to form chiral COFs.

Important factors affecting the formation of the high crystal structure of the COF, such as solvent, temperature, time and the amount of catalyst, were investigated in detail. Different solvents show different solubilities of the monomer, which in turn affects the formation of highly crystalline COFs in terms of the reaction rate. The combination of mesitylene and 1,4-dioxane was found to give the best crystalline COF (Fig. S7†). In addition, a composition of 5/5 (v/v) for the binary solvent of mesitylene and 1,4-dioxane resulted in the best crystallinity of TzDva (Fig. S8†). High temperature is not conducive to the formation of an ordered crystal structure of TzDva, so the TzDva synthesized at room temperature had a good crystal structure (Fig. S9†). The increase of the catalyst $Sc(OTf)_3$ content to 0.02 equiv. per aniline greatly enhanced the crystallinity of TzDva. An excessive catalyst loading (0.05 equiv.) made the crystallinity of TzDva decrease due to too fast reaction (Fig. S10†). A reaction time of 24 h was sufficient not only to generate crystalline frameworks as indicated by the significant increase of the peak intensity at 2.86° (Fig. S11†), but also to get a high yield of TzDva (Table S1†). As a result, TzDva powder with a yield of *ca.* 95.5% was synthesized from Tz and Dva in a mixture of mesitylene/1,4-dioxane (5/5, v/v) with $Sc(OTf)_3$ (0.02 equiv.) as the catalyst at room temperature for 24 h.

A crucial compromise between functionalization and crystallinity should be made in the post-synthesis of chiral COFs due to the effect of the introduced functional moiety into the framework on the properties of COFs such as porosity, crystallinity and surface area. We take the preparation of (*S*)-CTzDva as a proof of concept to demonstrate our strategy. The effect of the amount of (*S*)-*N*-(2-mercaptoethyl)-2-phenylpropanamide on the crystallinity and modification of (*S*)-CTzDva was studied (Table S2, Fig. S12†). Considering the sulfur content and crystallinity after modification, 50 mg (*S*)-*N*-(2-mercaptoethyl)-2-phenylpropanamide and 30 mg TzDva were selected to prepare (*S*)-CTzDva.

The crystal structures of the as-prepared TzDva and CTzDva were characterized by X-ray diffractometry and structural simulation. The PXRD pattern of the as-prepared TzDva exhibits several peaks at 2.86°, 4.98°, 5.69° and 7.47° (Fig. 2a and S13†), in good agreement with the simulated pattern in eclipsed AA stacking mode with the unit cell parameters $a = b = 36.2000$ Å, $c = 3.4000$ Å, $\alpha = \beta = 90°$ and $\gamma = 120°$ (Fig. 2a, and Table S3†). The experimental PXRD pattern matches well with the pattern of AA stacking mode after Pawley refinement with an R_{wp} of 4.87% and an R_p of 3.65% (Fig. S14†). Compared with TzDva, the introduction of (*R*)/(*S*)-*N*-(2-mercaptoethyl)-2-phenylpropanamide resulted in a significant reduction in the crystallinity of CTzDva (Fig. 2a and S13†).

The FT-IR spectra of TzDva exhibit a typical C=N stretching peak at 1605 cm^{-1}, indicating the successful formation of an imine bond (Fig. 2b and S15†). At the same time, the disappearance of the C=O stretching band (1687 cm^{-1}) of Dva and the stretching vibration band of the N–H bond of Tz (3300–3400 cm^{-1}) also shows the formation of imine bonds due to the condensation between the amino groups of Tz and the aldehyde groups of Dva. The FT-IR spectra of CTzDva (Fig. 2b and S15†) show a new –NH–CO– stretching peak at 1640 cm^{-1}, confirming

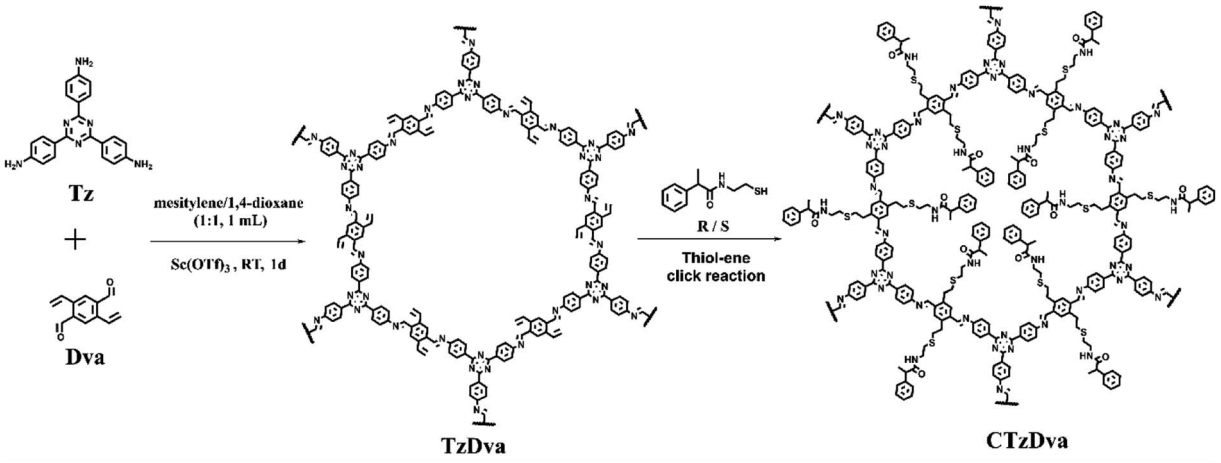

Fig. 1 Scheme for the synthesis of TzDva *via* the condensation of Tz and Dva, and CTzDva *via* the "thiol–ene" click reaction.

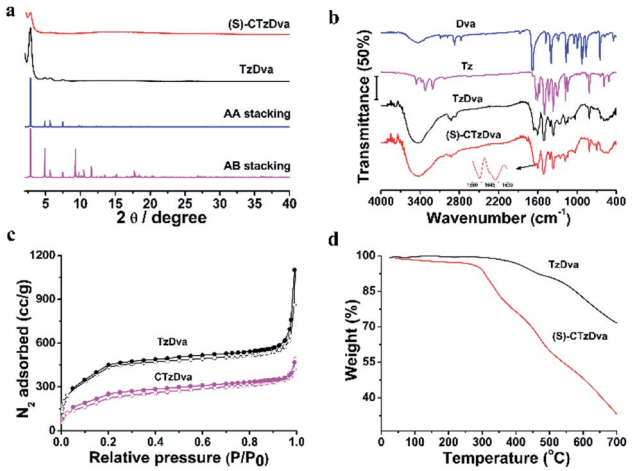

Fig. 2 (a) Experimental PXRD pattern of (*S*)-CTzDva (magenta line), experimental PXRD pattern of TzDva (black line), simulated PXRD patterns of TzDva for an AA eclipsed model (blue line) and AB staggered model (red line). (b) FT-IR spectra of Dva, Tz, TzDva and (*S*)-CTzDva. (c) N_2 adsorption–desorption isotherms of (*S*)-CTzDva and TzDva. (d) Thermogravimetric curves of (*S*)-CTzDva and TzDva.

the successful modification of (*R*)/(*S*)-*N*-(2-mercaptoethyl)-2-phenylpropionamide on the frameworks of TzDva. The sulfur signal at 163.5 eV in the XPS spectra of CTzDva can be attributed to (*R*)/(*S*)-*N*-(2-mercaptoethyl)-2-phenylpropionamide (Fig. S16†), and the presence of sulfur element further demonstrates the successful modification of (*S*)-*N*-(2-mercaptoethyl)-2-phenylpropionamide. The modification rate of chiral thiol derivatives on TzDva was *ca.* 69.0% according to XPS and elemental analysis.

The solid ^{13}C NMR spectrum further confirms the chemical structure of TzDva and CTzDva. The chemical shift of 160 ppm belongs to the characteristic peak of carbon atoms of the C=N bond formed by a Schiff reaction, which further proves the successful formation of imine bonds of TzDva (Fig. S17†). The ^{13}C solid NMR spectrum of CTzDva shows new characteristic peaks of the carbon atoms of C=O (190 ppm) and the characteristic peaks of the saturated alkane carbon atoms (60–10 ppm) (Fig. S18†). These characteristic peaks could be attributed to the carbon atoms on the chiral substance (*S*)-*N*-(2-mercaptoethyl)-2-phenylpropanamide. These results further confirm that (*S*)-*N*-(2-mertopyl-ethyl)-2-phenylpropanamide had successfully bonded to TzDva, and the introduction of chiral ligands did not change the framework structure of TzDva. CD spectra were further studied to characterize CTzDva (Fig. S19†). The CD spectrum of CTzDva shows a typical single curve, which proves the chirality of CTzDva.

The surface area and porosity of TzDva and CTzDva were characterized by N_2 adsorption–desorption measurements at 77 K. The Brunauer–Emmett–Teller (BET) surface area of TzDva was 1144 $m^2\ g^{-1}$, while the BET surface areas of CTzDva decreased to 524 $m^2\ g^{-1}$ (Fig. 2c) and 543 $m^2\ g^{-1}$ (Fig. S20†). Meanwhile, the pore size and pore volume of the COFs decreased from 28 Å and 0.903 $cm^3\ g^{-1}$ for TzDva to 12 Å and 0.533 $cm^3\ g^{-1}$ for (*S*)-CTzDva and 14 Å and 0.583 $cm^3\ g^{-1}$ for (*R*)-CTzDva, respectively (Fig. S21†). The morphology of TzDva and CTzDva was characterized by SEM and TEM. SEM and TEM images reveal the fiber morphology of TzDva and CTzDva, and the introduction of chiral groups onto the skeleton did not significantly change the morphology of TzDva (Fig. S22 and S23†).

The chemical stability of TzDva in conventional solvents was investigated by dispersing TzDva in different solvents at room temperature for 3 d. No significant change in the FT-IR and PXRD patterns was observed (Fig. S24 and S25†), indicating the good solvent stability of TzDva. Meanwhile, TzDva, (*S*)-CTzDva and (*R*)-CTzDva were relatively stable up to 320 °C, 280 °C and 260 °C (Fig. 2d and S26†), respectively.

Fabrication and characterization of COF coated capillaries

The CTzDva coated capillary column was prepared by a dynamic coating method. The SEM images of the CTzDva coated capillary column show that CTzDva was successfully coated on the capillary column (Fig. 3a and S27†). The appearance of the characteristic peaks of CTzDva at 1605 cm^{-1} (–C=N–) and

1653 cm^{-1} (–NH–CO–) in the FT-IR spectrum of the CTzDva coated capillary column reveals the successful preparation of the coated capillary column (Fig. 3b and S28†).

CTzDva coated capillaries for GC separation

The polarity of the capillary stationary phase is an important factor affecting GC separation. McReynolds constants were used to evaluate the polarity of the stationary phases TzDva and CTzDva (Table 1). The average McReynolds constants of the CTzDva stationary phase were 319 and 308, revealing a moderate polarity of the CTzDva coated capillary columns. The maximum McReynolds constant for Z (2-pentanone) among all the five test probes shows the strong polarizability and part of the dipolar character of the prepared CTzDva. In addition, the McReynolds constants for the U (nitropropane), Y (2-pentanone) and S (pyridine) components indicate that the prepared stationary has a moderate electron donating ability, hydrogen-bonding ability and acidic character.

The performance of the prepared CTzDva coated capillary was then demonstrated for GC separation of intractable analytes. The CTzDva coated capillary showed good ability for the separation of benzene and cyclohexane though the boiling point of cyclohexane (80.7 °C) is very close to that of benzene (80.1 °C) (Fig. S29†). The retention time of benzene was longer than that of cyclohexane, indicating that the adsorption of benzene was stronger than that of cyclohexane on CTzDva due to the π–π interaction between benzene and the aromatic walls of CTzDva.

The performance of the (*S*)-CTzDva coated capillary column was further revealed for the chiral separation of racemates. Two commercial chiral capillary columns (CycloSil B and CP-Chirasil Dex CB) were employed for comparison. As shown in Fig. 4a, the (*S*)-CTzDva coated capillary column shows good chiral separation for (±)-fenchone and (±)-citronellal within 5 minutes. (*S*)-CTzDva showed stronger retention of (−)-enantiomer than (+)-enantiomer. In contrast, (±)-citronellal were not separated on both commercial chiral capillary columns while (±)-fenchone were separated on the CP-Chirasil Dex CB within 28 min (Table S4,† Fig. 4b and c). The results show that the (*S*)-CTzDva coated capillary column has better chiral separation efficiency for (±)-fenchone and (±)-citronellal than the two commercial chiral capillary columns and faster chiral separation than the state-of-the-art polymers or porous materials (Table S4†).

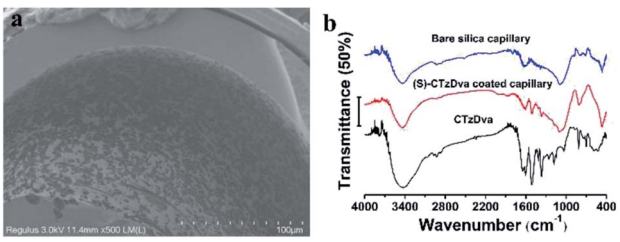

Fig. 3 Characterization of the (*S*)-CTzDva coated capillary column: (a) SEM images of the inner wall of the (*S*)-CTzDva coated capillary column. (b) FT-IR spectra of the bare silica capillary column, (*S*)-CTzDva coated capillary column and (*S*)-CTzDva powder.

Table 1 McReynolds constants of COF coated capillary columns[a]

Column	X	Y	Z	U	S	Av.
TzDva	18	177	107	79	93	95
(*S*)-CTzDva	206	315	407	374	294	319
(*R*)-CTzDva	201	291	397	367	286	308

[a] Measured at 100 °C. X, Y, Z, U and S refer to benzene, butanol, 2-pentanone, nitropropane and pyridine, respectively.

To further investigate the role of the chiral microenvironment, two additional COFs (*R*)-CTzDva and (*RS*)-TzDva were prepared *via* post-modification with the *R*-configuration of the chiral ligand and racemic chiral ligand, respectively (Fig. S30–S35†). For comparison, capillary columns coated with (*R*)-CTzDva and (*RS*)-TzDva were also prepared, respectively. Besides (*S*)-CTzDva, the (*R*)-CTzDva coated capillary column also gave good chiral separation of (±)-fenchone and (±)-citronellal but with a reversed retention order for the two enantiomers on the (*S*)-CTzDva coated capillary column, whereas the (*RS*)-TzDva coated column showed no chiral separation (Fig. S36 and S37†). The results show the important roles of the chiral microenvironment in chiral separation.[39,40]

To show the importance of the specific frameworks of CTzDva in chiral separation, an *S*-configuration chiral ligand functionalized capillary column was further prepared for

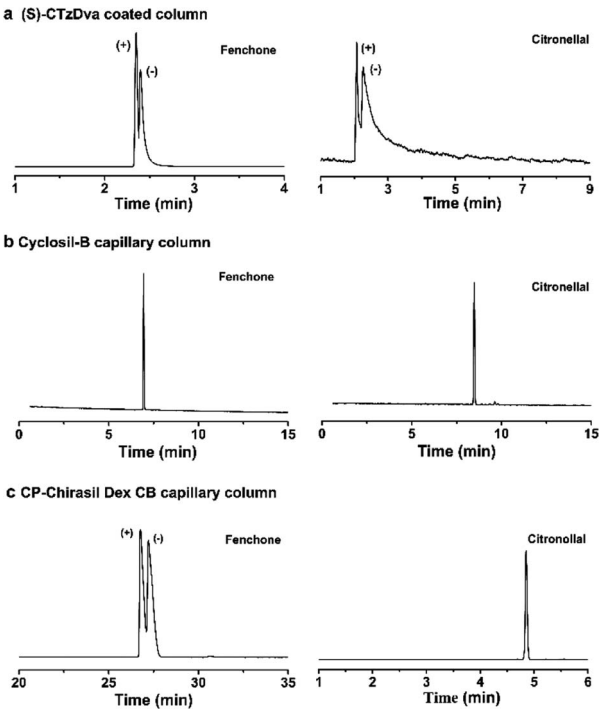

Fig. 4 Separation of racemates: (a) (*S*)-CTzDva coated column (30 m long, 0.32 mm i.d.): fenchone (150 °C, 1 mL min^{-1}) and citronellal (160 °C, 1 mL min^{-1}). (b) Cyclosil-B capillary column (30 m long, 0.25 mm i.d.): fenchone (150 °C, 1 mL min^{-1}) and citronellal (160 °C, 1 mL min^{-1}). (c) CP-Chirasil Dex CB capillary column (25 m long, 0.25 mm i.d.): fenchone (100 °C, 1 mL min^{-1}) and (b) citronellal (160 °C, 1 mL min^{-1}).

comparison. Although this column had a similar chiral microenvironment to the (*S*)-CTzDva coated column, it gave no separation of the racemates (Fig. S38†) as (*RS*)-TzDva (Fig. S37†) or TzDva coated columns (Fig. S39†). The results confirm that only the chiral microenvironment of the chiral ligand or the specific frameworks of COF TzDva cannot give chiral separation. Therefore, it is the synergistic effect of the chiral microenvironment of the chiral ligand and the specific frameworks of COF TzDva that accounts for the chiral separation on the CTzDva coated column. The kinetic diameters of fenchone and citronellal are smaller than the pore size of CTzDva (Fig. S40†), so we assume that the chiral separation mainly occurred inside the pore of CTzDva. Other interactions such as π–π interaction and hydrogen-bonding provided by CTzDva also play important roles in chiral chromatographic separation.[28,41]

The repeatability and reproducibility of the (*S*)-CTzDva coated capillary column were explored. The relative standard deviations (RSDs) of the retention time for run to run ($n = 7$) and day to day ($n = 5$) were 0.2–0.7% and 0.5–2.2%, respectively, which demonstrates the good repeatability of the (*S*)-CTzDva coated capillary columns (Table S5†).

Conclusions

In summary, we have reported a facile "thiol–ene" click strategy to prepare chiral COFs and the application of CTzDva as a novel chiral stationary phase to fabricate a CTzDva coated capillary column for GC. The prepared chiral COF CTzDva exhibits high thermal stability and a large surface area, while CTzDva coated capillary columns show good resolution for the separation of benzene/cyclohexane and enantiomers. This work provides a convenient strategy for the preparation of chiral COFs for the separation of racemates.

Author contributions

Jing-Xuan Guo: conceptualization, investigation, data curation, validation, and writing-original draft. Cheng Yang: validation. Xiu-Ping Yan: conceptualization, project administration, writing-review & editing, funding acquisition, and supervision.

Conflicts of interest

There are no conflicts to declare.

Acknowledgements

This work was supported by the National Natural Science Foundation of China (No. 21775056), the National First-class Discipline Program of Food Science and Technology (No. JUFSTR20180301), and the Collaborative Innovation Center of Food Safety and Quality Control in Jiangsu Province.

Notes and references

1 A. P. Cote, A. I. Benin, N. W. Ockwig, M. O'Keeffe, A. J. Matzger and O. M. Yaghi, *Science*, 2005, **310**, 1166–1170.
2 P. J. Waller, F. Gándara and O. M. Yaghi, *Acc. Chem. Res.*, 2015, **48**, 3053–3063.
3 E. L. Spitler and W. R. Dichtel, *Nat. Chem.*, 2010, **2**, 672–677.
4 S. Kandambeth, D. B. Shinde, M. K. Panda, B. Lukose, T. Heine and R. Banerjee, *Angew. Chem., Int. Ed.*, 2013, **125**, 13290–13294.
5 N. Huang, P. Wang and D. L. Jiang, *Nat. Rev. Mater.*, 2016, **1**, 1–19.
6 K. Y. Geng, T. He, R. Y. Liu, S. Dalapati, K. T. Tan, Z. P. Li, S. S. Tao, Y. F. Gong, Q. H. Jiang and D. L. Jiang, *Chem. Rev.*, 2020, **120**, 8814–8933.
7 Y. Zhi, P. Shao, X. Feng, H. Xia, Y. Zhang, Z. Shi, Y. Mu and X. Liu, *J. Mater. Chem. A*, 2018, **6**, 374–382.
8 Y. Zeng, R. Zou and Y. Zhao, *Adv. Mater.*, 2016, **28**, 2855–2873.
9 S. Lin, C. S. Diercks, Y.-B. Zhang, N. Kornienko, E. M. Nichols, Y. Zhao, A. R. Pairs, D. Kim, P. Yang and O. M. Yaghi, *Science*, 2015, **349**, 1208–1213.
10 S.-Y. Ding, J. Gao, Q. Wang, Y. Zhang, W.-G. Song, C.-Y. Su and W. Wang, *J. Am. Chem. Soc.*, 2011, **133**, 19816–19822.
11 X. Wu, X. Han, Q. S. Xu, Y. H. Liu, C. Yuan, S. Yang, Y. Liu, J. W. Jiang and Y. Cui, *J. Am. Chem. Soc.*, 2019, **141**, 7081–7089.
12 M.-W. Zhu, S.-Q. Xu, X.-Z. Wang, Y. Chen, L. Dai and X. Zhao, *Chem. Commun.*, 2018, **54**, 2308–2311.
13 Q. Fang, J. Wang, S. Gu, R. B. Kaspar, Z. Zhuang, J. Zheng, H. Guo, S. Qiu and Y. Yan, *J. Am. Chem. Soc.*, 2015, **137**, 8352–8355.
14 G. Zhang, X. Li, Q. Liao, Y. Liu, K. Xi, W. Huang and X. Jia, *Nat. Commun.*, 2018, **9**, 2785.
15 Z. Wang, S. Zhang, Y. Chen, Z. Zhang and S. Ma, *Chem. Soc. Rev.*, 2020, **49**, 708–735.
16 C. X. Yang, C. Liu, Y. M. Cao and X. P. Yan, *Chem. Commun.*, 2015, **51**, 12254–12257.
17 K. Dey, M. Pal, K. C. Rout, K. H. Shebeeb, A. Das, R. Mukherjee, U. K. Kharul and R. Banerjee, *J. Am. Chem. Soc.*, 2017, **139**, 13083–13091.
18 J. Huang, X. Han, S. Yang, Y. Cao, C. Yuan, Y. Liu, J. Wang and Y. Cui, *J. Am. Chem. Soc.*, 2019, **141**, 8996–9003.
19 H. Yang, L. Yang, H. Wang, Z. Xu and Z. Jiang, *Nat. Commun.*, 2019, **10**, 2101.
20 M. Zhang, X. L. Chen, J. H. Zhang, J. Kong and L. M. Yuan, *Chirality*, 2016, **28**, 340–346.
21 Y. Liu, W. M. Xuan and Y. Cui, *Adv. Mater.*, 2010, **22**, 4112–4135.
22 W. T. Kou, C. X. Yang and X. P. Yan, *J. Mater. Chem. A*, 2018, **6**, 17861–17866.
23 M. Zhang, Z. J. Pu, X. L. Chen, X. L. Gong, A. X. Zhu and L. M. Yuan, *Chem. Commun.*, 2013, **49**, 5201–5203.
24 S. M. Xie, X. H. Zhang, Z. J. Zhang, M. Zhang, J. Jia and L. M. Yuan, *Anal. Bioanal. Chem.*, 2013, **405**, 3407–3412.
25 X. Kuang, Y. Ma, H. Su, J. Zhang, Y. B. Dong and B. Tang, *Anal. Chem.*, 2014, **86**, 1277–1281.
26 J. Dong, Y. Liu and Y. Cui, *Chem. Commun.*, 2014, **50**, 14949–14952.
27 P. Sun and D. W. Armstrong, *J. Chromatogra. A*, 2010, **1217**, 4904–4918.

28 H. L. Qian, C. X. Yang and X. P. Yan, *Nat. Commun.*, 2016, **7**, 12104.
29 S. Zhang, Y. Zheng, H. An, B. Aguila, C. Yang, Y. Dong, W. Xie, P. Cheng, Z. Zhang, Y. Chen and S. Ma, *Angew. Chem., Int. Ed.*, 2018, **57**, 16754–16759.
30 X. Han, J. Huang, C. Yuan, Y. Liu and Y. Cui, *J. Am. Chem. Soc.*, 2018, **140**, 892–895.
31 G. Liu, J. Sheng and Y. Zhao, *Sci. China Chem.*, 2017, **60**, 1015–1020.
32 Y. Du, K. Mao, P. Kamakoti, P. Ravikovitch, C. Paur, S. Cundy, Q. Li and D. Calabro, *Chem. Commun.*, 2012, **48**, 4606–4608.
33 J. L. Segura, S. Royuela and M. M. Ramos, *Chem. Soc. Rev.*, 2019, **48**, 3903–3945.
34 H. Ding, A. Mal and C. Wang, *Mater. Chem. Front.*, 2020, **4**, 113–127.
35 C. E. Hoyle and C. N. Bowman, *Angew. Chem., Int. Ed.*, 2010, **49**, 1540–1573.
36 A. B. Lowe, *Polym. Chem.*, 2010, **1**, 17–36.
37 D. P. Nair, M. Podgórski, S. Chatani, T. Gong, W. Xi, C. R. Fenoli and C. N. Bowman, *Chem. Mater.*, 2014, **26**, 724–744.
38 F. Dénès, M. Pichowicz, G. Povie and P. Renaud, *Chem. Rev.*, 2014, **114**, 2587–2693.
39 D. W. Armstrong, T. J. Ward, R. D. Armstrong and T. E. Beesley, *Science*, 1986, **232**, 1132–1135.
40 C. Yamamoto, E. Yashima and Y. Okamoto, *J. Am. Chem. Soc.*, 2002, **124**, 12583–12589.
41 G. K. E. Scriba, *Chromatographia*, 2012, **75**, 815–838.